

LONGITUDINAL SPACE CHARGE IN THE SLC, FFTB AND NLC FINAL-FOCUS SYSTEMS*

F. Zimmermann and T. O. Raubenheimer, SLAC, Stanford, CA 94309, USA

Abstract

In a final-focus system, space-charge forces can be significant even for very high beam energies. The reason is the inherent large chromaticity of such a system, which needs to be compensated to a high precision. The longitudinal space-charge force causes an energy variation along the bunch, which depends on beam size, beam-pipe radius, and bunch population. Since this energy variation is location-dependent, it may affect the chromatic correction and, thereby, increase the IP spot size. The space-charge force then gives rise to a limit on bunch intensity beyond which the resulting spot-size increase will degrade the final-focus performance. In this paper, the effect of longitudinal space charge is evaluated and intensity limits are derived for three existing or proposed final foci.

1 INTRODUCTION

The purpose of a final-focus system for a linear collider is to demagnify a high-energetic electron (or positron) beam to a minuscule vertical spot size at the interaction point (IP). The last focusing before the IP is achieved with two or three strong quadrupoles, a so-called final doublet or triplet. At these quadrupoles the values of the beta functions are huge, up to tens or hundreds of kilometers, and, as a result, the system is highly chromatic. The chromaticity is conventionally canceled by upstream sextupole magnets at locations with nonzero dispersion. In order to achieve the desired small spot sizes at the IP, the chromaticity needs to be compensated very accurately for all particles in a bunch. Small changes to the energy distribution inside a bunch which occur between sextupoles and final quadrupoles may impair the chromatic correction, and may lead to an increase of the IP spot size. More specifically, the chromatic contribution to the vertical spot size at the IP can be written

$$\frac{\Delta\sigma_y}{\sigma_y} = \xi \Delta\delta_{rms} \quad (1)$$

where the dimensionless number ξ characterizes the (vertical) chromaticity of the final transformer, and $\Delta\delta_{rms}$ denotes the rms difference of the particle-energies at sextupoles and final quadrupoles, divided by the average beam energy E_b . The term $\Delta\sigma_y$ of Eq. (1) has to be added in quadrature to the design spot size. As an example, $\xi \approx 6000$ in the SLC final focus, $\xi \approx 26\,000$ for the FFTB, and $\xi \approx 32\,000$ for the NLC, and, thus, the rms energy difference between sextupoles and final quadrupoles at which

the total spot size increases by 2% is

$$\Delta\delta_{rms} \leq \begin{cases} 3 \times 10^{-5} & \text{(SLC)} \\ 8 \times 10^{-6} & \text{(FFTB)} \\ 6 \times 10^{-6} & \text{(NLC)} \end{cases} \quad (2)$$

These are very small numbers—orders of magnitude smaller than the beam energy spread. They reflect the sensitivity of the spot size to energy variations inside a bunch which are generated in the final focus itself. A harmful energy variation $\Delta\delta_{rms}$ can be caused by forces so small that they might completely be ignored, in view of the high beam energy, if they would not affect the chromatic correction. In this paper, we consider one such potentially harmful force, the longitudinal space charge, and evaluate its importance for the SLC, FFTB and NLC final-focus systems. The longitudinal space-charge force also changes the average beam energy at the IP, which could be important for the correct analysis of high-precision physics experiments. Finally, we note that the wake-field induced by beam-pipe discontinuities results in an additional energy variation, which may either counteract or enhance the space-charge effect and which is not included in the following analysis.

2 LONGITUDINAL SPACE CHARGE

The space-charge force causes both an energy shift and an energy variation along the bunch, which depend on beam size, beam-pipe radius, and bunch population. We will neglect the contribution to the space-charge force which arises from the nonuniformity of the longitudinal distribution, since it is suppressed by $1/\gamma^2$, where γ denotes the relativistic Lorentz factor. As discussed in the introduction, the space-charge induced energy variation changes with location and, thus, may affect the chromatic correction. Because it is intensity-dependent, a limit on the bunch intensity exists beyond which the resulting spot-size increase will degrade the final-focus performance. An estimate of the critical intensity is obtained by comparing typical values for $\Delta\delta_{rms}$ with Eq. (2). To this end, we consider an ultrarelativistic electron (or positron) bunch traversing at the center of a perfectly conducting circular beam pipe, whose electrostatic potential is assumed to be zero. If the transverse beam distribution is Gaussian, the potential energy $\Phi(x, y, z)$ of a particle on the beam axis ($x, y=0$) is

$$e\Phi(0, 0, z) = \frac{e\lambda(z)}{4\pi\epsilon_0} \left(C + \ln 2 - 2 \ln \left(\frac{\sigma_x + \sigma_y}{R} \right) \right) \quad (3)$$

where $C \approx 0.577\dots$ denotes Euler's constant, e the electron charge, R is the beam-pipe radius, σ_x and σ_y

* Work supported by the Department of Energy, contract DE-AC03-76SF00515

are the horizontal and vertical rms beam sizes, respectively, and λ is the charge line density at longitudinal position z within the bunch. Assuming the longitudinal distribution is also Gaussian, we have $\lambda(z) = Ne/(\sqrt{2\pi}\sigma_z) \exp(-z^2/(2\sigma_z^2))$, where N is the number of particles per bunch. For the NLC, we find $\lambda(0) \approx 5 \times 10^{-6}$ C/m, for the FFTB $\lambda(0) \approx 1 \times 10^{-6}$ C/m, and for the SLC $\lambda(0) \approx 4 \times 10^{-6}$ C/m. The change of the kinetic energy between two locations (1 and 2) for an on-axis particle at position z is given by Eq. (3). Since a change of the average bunch energy is easily corrected by adjusting the magnet strengths, it is the spread of energy change, i.e. the rms change, which is harmful. Both energy changes can be estimated from the z -dependence of $\Phi(z, 0)$,

$$\begin{pmatrix} \Delta\delta_{rms} \\ \Delta\delta_{ave} \end{pmatrix} \approx \begin{pmatrix} 0.28 \\ 0.71 \end{pmatrix} \frac{2Nr_e}{\sqrt{2\pi}\sigma_z\gamma} \ln\left(\frac{\sigma_{sum,2}R_1}{\sigma_{sum,1}R_2}\right) \quad (4)$$

where $\sigma_{sum} \equiv \sigma_x + \sigma_y$ denotes the sum of the two transverse rms sizes, and r_e the classical electron radius. We have used $\lambda_{rms} \approx (1/\sqrt{3} - 1/2)^{1/2} \times \lambda(0)$ and $\lambda_{ave} \approx 1/\sqrt{2} \times \lambda(0)$. Note that, in Eq. (4), we have ignored the dependence of the potential on the transverse position.

For the SLC, we have $\sigma_{sum} \approx 1.71$ mm inside Q2, the center magnet of the final triplet, and $\sigma_{sum} \approx 850$ μm at the Y-sextupoles. The beam pipe radius in sextupoles and final quadrupoles is about the same. In the FFTB the beam size at the Y-sextupoles, $\sigma_{sum} \approx 650$ μm , almost equals that at the center of the final quadrupole $\sigma_{sum} \approx 570$ μm . Finally, for the 500-GeV c.m.-energy NLC design, the beam sizes are $\sigma_{sum} \approx 337$ μm at the Y-sextupoles and $\sigma_{sum} \approx 250$ μm inside the first quadrupole Q1. Assuming typical operating or design currents (4×10^{10} , 10^{10} and 0.65×10^{10} particles per bunch, respectively) and bunch lengths of 700 μm , 600 μm , and 100 μm , the rms energy difference between sextupoles and final quadrupoles is

$$\Delta\delta_{rms} \approx \begin{cases} 2.5 \times 10^{-7} & \text{(SLC)} \\ 1.4 \times 10^{-8} & \text{(FFTB)} \\ 2.5 \times 10^{-8} & \text{(NLC)} \end{cases} \quad (5)$$

Using Eq. (2), the critical current for a 2% spot size increase is estimated to be more than an order of magnitude larger than the present design or operating current. This is a crude estimate, since the beam sizes inside the final quadrupoles change rapidly, the chromaticity of other final-focus magnets has been neglected, and we have ignored the dependence of the potential on the transverse coordinates.

We can also estimate the change of the beam energy at the IP. In the SLC, the IP beam size is 2 $\mu\text{m} \times 500$ nm; the NLC is designed for a spot size of 300 nm \times 4.5 nm. These numbers imply a change of the average beam energy at the IP, relative to that inside the last quadrupoles, by

$$\Delta E \approx \begin{cases} -280 \text{ keV} & \triangleq -6.0 \times 10^{-6} & \text{(SLC)} \\ -350 \text{ keV} & \triangleq -1.4 \times 10^{-6} & \text{(NLC)} \end{cases} \quad (6)$$

which is more than hundred times smaller than the rms energy spread of the beam and most likely insignificant.

To study the space-charge induced spot-size increase and the IP energy change in more detail, and to improve

the above estimates, we have modified the multi-particle tracking code MAD [1] so as to include the energy variation due to space charge. In the simulation, the space-charge force is calculated solely from the change of the transverse beam dimensions, since, for the systems considered, the beam-pipe aperture variation is not very important.

Apart from an arbitrary additive constant, the electrostatic potential of a Gaussian charge distribution, with transverse rms sizes σ_x and σ_y , reads [2]

$$\Phi(x, y, z) = \frac{\lambda(z)}{4\pi\epsilon_0} \int_0^\infty \frac{e^{-\frac{x^2}{2\sigma_x^2+q} + \frac{y^2}{2\sigma_y^2+q}}}{\sqrt{2\sigma_x^2+q}\sqrt{2\sigma_y^2+q}} dq. \quad (7)$$

Assuming σ_x and σ_y are slowly varying with location s , the potential $\Phi(x, y, z, s)$ satisfies the differential equation

$$\frac{\partial\Phi}{\partial s} \approx \frac{1}{2} \frac{d\sigma_x^2}{ds} \frac{\partial^2\Phi}{\partial x^2} + \frac{1}{2} \frac{d\sigma_y^2}{ds} \frac{\partial^2\Phi}{\partial y^2}. \quad (8)$$

which shows that the longitudinal space-charge force F_s ($= -e\partial\Phi/\partial s$) can be expressed in terms of the derivative of the transverse forces $F_{x,y}$ as follows:

$$\begin{aligned} F_s &\approx \frac{1}{2} \frac{d\sigma_x^2}{ds} \frac{\partial F_x}{\partial x} + \frac{1}{2} \frac{d\sigma_y^2}{ds} \frac{\partial F_y}{\partial y} \\ &= [-\alpha_x \epsilon_x + \eta_x \eta'_x \sigma_\delta^2] \frac{\partial F_x}{\partial x} - \alpha_y \epsilon_y \frac{\partial F_y}{\partial y} \end{aligned} \quad (9)$$

In the simulation, a multi-particle distribution is propagated step by step through the magnets and drift spaces of the final-focus system. After each step, of length Δs , the relative energy deviation δ of a particle with coordinates x, y and z is changed by an amount $\Delta\delta$ which, for a flat beam ($\sigma_x \gg \sigma_y$), reads

$$\begin{aligned} \Delta\delta(x, y, z) &= \Delta s \cdot \frac{\lambda(z)r_e}{\gamma} \left(\frac{2\pi}{\sigma_x^2 - \sigma_y^2}\right)^{1/2} \left[-\alpha_y \epsilon_y \frac{\partial}{\partial y} \right. \\ &\quad \left. \text{Re } \mathcal{F}(x, y) + (-\alpha_x \epsilon_x + \eta_x \eta'_x \sigma_\delta^2) \frac{\partial}{\partial x} \text{Im } \mathcal{F}(x, y) \right] \end{aligned}$$

where σ_x and σ_y denote the rms beam sizes at location s , and $\mathcal{F}(x, y)$ is defined in terms of the complex error function W as

$$\begin{aligned} \mathcal{F}(x, y) &= W\left(\frac{x + iy}{(2(\sigma_x^2 - \sigma_y^2))^{1/2}}\right) \\ &\quad - e^{-\frac{x^2}{2\sigma_x^2} - \frac{y^2}{2\sigma_y^2}} W\left(\frac{\frac{\sigma_y}{\sigma_x}x + i\frac{\sigma_x}{\sigma_y}y}{(2(\sigma_x^2 - \sigma_y^2))^{1/2}}\right). \end{aligned}$$

The function \mathcal{F} is familiar from the Bassetti-Erskine representation for the transverse fields of a Gaussian charge distribution [3]. If $\sigma_y \gg \sigma_x$, the coordinates x and y in Eq. (10) need to be interchanged. Finally, to avoid singularities, if $\sigma_x \approx \sigma_y$, the electrostatic force of a round beam is used for $F_{x,y}$ in Eq. (9). It is notable that for small amplitudes ($x/\sigma_x \lesssim 1, y/\sigma_y \lesssim 1$) the energy change for both flat and round beams simplifies to

$$\Delta\delta(z) \approx -\frac{\Delta s 2\lambda(z)r_e}{\gamma(\sigma_x + \sigma_y)} \left[\frac{\alpha_y \epsilon_y}{\sigma_y} + \frac{\alpha_x \epsilon_x - \eta_x \eta'_x \sigma_\delta^2}{\sigma_x} \right]$$

which is independent of the transverse position.

Typical tracking results including space charge are presented in Figs. 1–3, and in Table 1. Figures 1 and 2 display the variation of the average bunch energy along the NLC and SLC final foci, respectively. The magnitude of the energy variation is consistent with our earlier estimates. It seems fortuitous that, in both systems, the energy difference between sextupoles and the last quadrupoles is much smaller than the 'typical' energy variation. Figure 3 depicts the energy variation in an odd-dispersion final focus, designed by Oide [4], for roughly the same IP beam parameters as in Fig. 1. In this system only the second Y-sextupole is used for chromatic correction. This particular odd-dispersion design is slightly more sensitive to space charge than the design of Fig. 1, although the effect is still small.

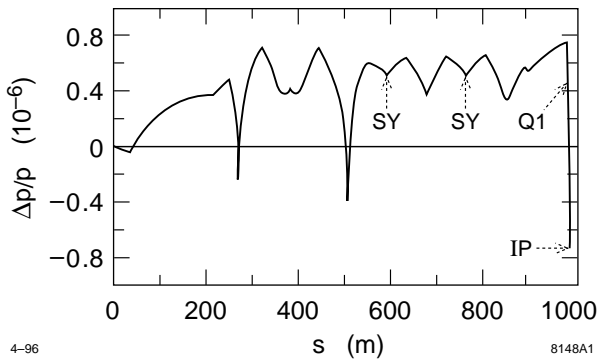


Figure 1: Variation of average bunch energy due to the longitudinal space-charge force in a 500 GeV c.m.-energy NLC final focus system, for a bunch length of $100 \mu\text{m}$ and 6.5×10^9 particles per bunch.

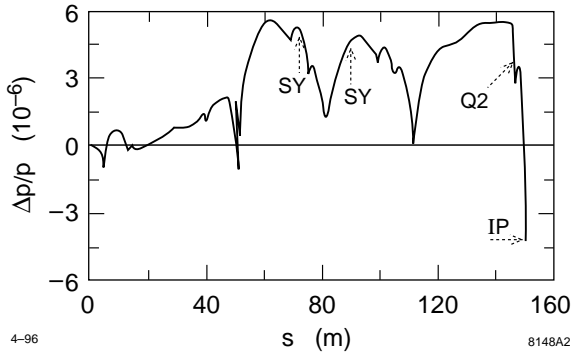


Figure 2: Variation of average bunch energy due to longitudinal space-charge force in the SLC final focus system, for a bunch length of $700 \mu\text{m}$ and 4×10^{10} particles per bunch.

Table 1 lists exemplary spot-size increases obtained by multi-particle tracking. The spot sizes change sensibly for bunch populations larger than a few times 10^{11} particles. As expected from Eqs. (1) and (4), the relative spot-size increase (to be added in quadrature) is proportional to the beam intensity. In the simulation, no attempt was made to correct for the change of average beam energy. Thus, the real intensity limit will be about two times higher than

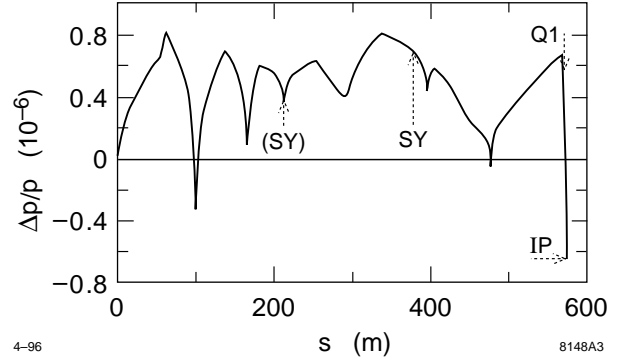


Figure 3: Variation of average bunch energy due to longitudinal space-charge force in a 500-GeV c.m.-energy odd-dispersion final focus system. Beam parameters are the same as in Fig. 1.

that predicted by Table 1, if we assume that the magnet strengths will be adapted to the actual local beam energy.

N	$\Delta\sigma_y/\sigma_{y0}$			
	SLC	FFTB	NLC	odd- η NLC
1×10^{11}	5.1%	0.3%	8.4%	15.7%
2×10^{11}	9.8%	0.6%	24.6%	30.9%
4×10^{11}	17.4%	1.3%	55.5%	61.2%

Table 1: Simulated relative increase of the vertical spot size due to longitudinal space charge, for different numbers of particles per bunch N . The design spot sizes σ_{y0} are 370 nm, 44 nm and 4.5 nm, for SLC, FFTB and NLC, respectively, to which the contribution $\Delta\sigma_y$ has to be added in quadrature.

3 CONCLUSION

Longitudinal space charge in the final-focus system places a limit on the achievable luminosity of a linear collider. For the NLC, FFTB and SLC final foci, space-charge forces were found to be significant for bunch populations an order of magnitude larger than their design or operating value. For a different final-focus optics the critical intensity could be considerably lower and, therefore, the space-charge effect deserves some attention during the design phase. In addition to the spot-size increase, the space-charge force also causes a change of the average beam energy at the IP, which, although rather small, might prove important in the analysis of high-precision experiments.

4 REFERENCES

- [1] H. Grote and F. C. Iselin, CERN/SL/90-13 (AP) (1990).
- [2] S. Kheifets, PETRA Note 119 (1976).
- [3] M. Bassetti, G. A. Erskine, CERN-ISR-TH/80-06 (1980).
- [4] K. Oide, HEACC 92, Hamburg, p. 861 (1992).